Princeton Plasma Physics Laboratory

PPPL- 5005

PPPL- 5005

Electromagnetic Analysis For The Design Of ITER Diagnostic Port Plugs During Plasma Disruptions

Y. Zhai, R. Federe, A. Brooks, M. Ulrickson,
C.S. Pitcher and G.D. Loesser

MARCH, 2014

PPPL PRINCETON PLASMA PHYSICS LABORATORY

Prepared for the U.S. Department of Energy under Contract DE-AC02-09CH11466.

Princeton Plasma Physics Laboratory
Report Disclaimers

Full Legal Disclaimer

Trademark Disclaimer

PPPL Report Availability

Princeton Plasma Physics Laboratory:

http://www.pppl.gov/techreports.cfm

Office of Scientific and Technical Information (OSTI):

http://www.osti.gov/bridge

Related Links:

U.S. Department of Energy

Office of Scientific and Technical Information

Fusion Links

Electromagnetic Analysis for the Design of ITER Diagnostic Port Plugs during Plasma Disruptions

Y. Zhai[1,a], R. Feder[1], A. Brooks[1], M. Ulrickson[2], C. S. Pitcher[3], G. D. Loesser[1]

[1]*Princeton Plasma Physics Laboratory, Princeton, NJ, USA*
[2]*Sandia National Laboratory, Albuquerque, NM, USA*
[3]*ITER Organization, Route de Vinon sur Verdon, St Paul lez Durance, France*

ITER diagnostic port plugs perform many functions including structural support of diagnostic systems under high electromagnetic loads while allowing for diagnostic access to the plasma. The design of diagnostic equatorial port plugs (EPP) are largely driven by electromagnetic loads and associate responses of EPP structure during plasma disruptions and VDEs. This paper summarizes results of transient electromagnetic analysis using Opera 3d in support of the design activities for ITER diagnostic EPP. A complete distribution of disruption loads on the Diagnostic First Walls (DFWs), Diagnostic Shield Modules (DSMs) and the EPP structure, as well as impact on the system design integration due to electrical contact among various EPP structural components are discussed.

I. INTRODUCTION

ITER diagnostic port plugs perform many functions including structural support of diagnostic systems under high electromagnetic loads while allowing for diagnostic access to the plasma [1-3]. Each water cooled generic port plug structure is filled with customized shielding and diagnostic equipment. The design of diagnostic equatorial port plugs (EPP) are largely driven by the electromagnetic loads and the associate responses of EPP structural components during fast plasma disruptions and VDEs [1, 4]. To mitigate the large disruption loads, the design of diagnostic EPP has changed from the horizontal drawer configuration during conceptual design phase to a vertical drawer configuration in the preliminary design [4] to effectively cut eddy current flowing paths on the EPP diagnostic drawers. As a result, a factor of 2-3 reduction of disruption loads brought down the maximum deflection of EPP structure during disruptions to <5 mm and the dynamic response of the EPP structure on the vacuum vessel becomes manageable. Although the upward major disruption with 36 ms linear current decay produces the largest radial moments and radial forces on the diagnostic first walls (DFWs), diagnostic shield modules (DSMs) and the EPP structure, other disruption cases or VDEs can produce larger minority disruption loads such as the poloidal moment and force. Electrical contact between DFWs and DSMs will also have a significant impact on the EM load distribution and thus affects the design of the DFW attachment scheme. Large current transfer (~160 kA) between DFWs and DSMs through the attachment keys and pads during disruption implies local heating and potential welding. A complete distribution of disruption loads on the EPP structure and the associate responses, as well as the impact on system design integration due to electrical contact among various structural components will be discussed.

Early design studies show that electrical contact between the DSMs and the port plug structure may increase ~10-20% the net disruption loads on the full EPP structure [4]. The IO vertical drawer model includes a 5 mm gap between the front face of the EPP structure and the DSM. There will still be eddy current flowing between DSM and EPP structure through the rails and the DSM water pipes. To avoid potential arcing and welding, detailed analysis is performed to identify major eddy current loops and thus to quantify the current and voltages involved for potential arcing; also to extract disruption loads on the DFW and DSM cooling water pipes.

II. Model Description

A 20 degree sector of the ITER vacuum vessel (VV), the IO diagnostic vertical drawers with neighboring Blanket Shield Modules (BSMs), and the EPP structure is modeled in Opera 3d, a commercial electromagnetic analysis tool. The cyclic symmetric model uses the 3D Elecktra transient analysis capability of Opera 3d for the solution of eddy current problems on the EPP. Figure 1 presents the cutaway view of coils and plasma filaments modeled as secondary excitations. The central or vertical machine axis is aligned with the ITER global z axis. The machine mid-plane is on the X-Y plane with the X axis pointing to the radial direction. The 20-degree cut planes are symmetric around the vertical central X-Z plane. The EPP is 10 degrees off from the global X axis. A positive rotational symmetry around the global Z axis is applied to the Opera model with a total of 18 symmetry copies.

The 6 CS, 6 PF and 18 TF coil configuration is used to provide the static background field for force calculations during major disruptions. The ITER sign and direction convention is used so that plasma current and toroidal field are clockwise (-) but most CS and PF coils are counterclockwise (+). The plasma modeling based on the plasma simulation code DINA 2010 provides a transient history of plasma-induced flux change, a source excitation of eddy current in the model. The IO DINA 2010 data sets with 64 secondary excitations are used to model all plasma current drivers. The toroidal flux drivers are not

included as previous analysis indicated that it has a small impact on the EPP structure but will significantly increase the model run time [5]. The Halo current effect is also neglected since the present design of the EPP has 10 cm setback of the plasma-facing front face enforced to minimize this effect [1].

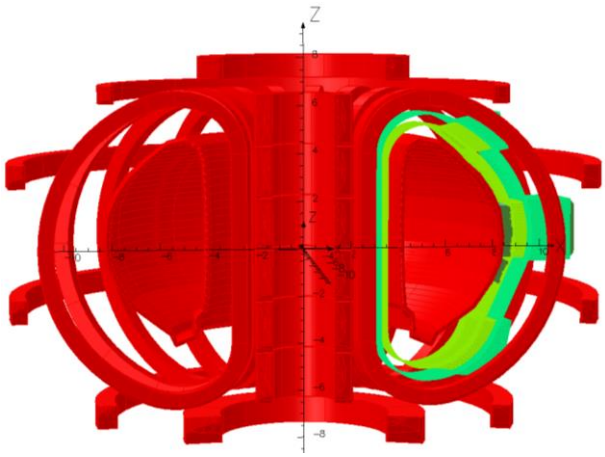

Figure 1 Cutaway view of the ITER coils and plasma filaments with a 20 degree model of VV and Diagnostic EPP (cyclic symmetry)

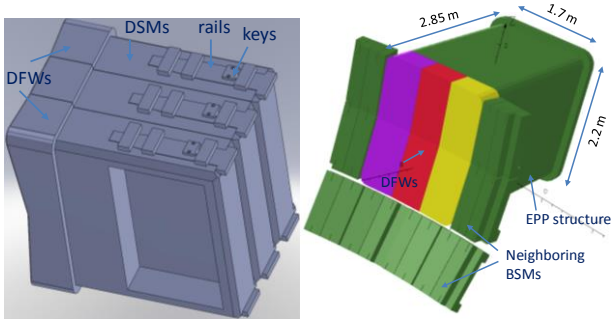

Figure 2 Vertical drawers and support rails (left) and Opera 3d model with the neighboring BSMs (right) of diagnostic equatorial port plug

The background fields are benchmarked against results from ANSYS EMAG and Maxwell with generally ~3% difference. Figure 2 presents the IO vertical drawer model with rails and Opera 3d model with neighboring BSMs. The upper neighboring BSM is not included here due to meshing difficulty. Results from models including the upper neighboring BSM show only ~1% difference in net moment on the full EPP structure. This is mainly because fields from sliced neighboring BSMs are small compared to background fields and fields from other eddy currents in VV, DFWs and DSMs. Table 1 presents the material conductivities used in the Opera 3d model.

Table 1 Electrical conductivity of the EPP structures

	Conductivity (S/m)
DFWs/DSMs	1.08×10^6 (80% SS)
Bolts/Pads/Rails	1.35×10^6 (SS)
VV and EPP Structure	1.35×10^6 (SS)

III. Disruption Scenarios

Disruption cases listed in Table 2 are studied following IO requirements for CDR and PDR.

Table 2 Selected Disruption Scenarios

VDE_UP_LIN36	VDE III (no VDE IV)	Level C
VDE_DW_LIN36	VDE III (no VDE IV)	Level C
MD_UP_LIN36	MD II (no MD III or MD IV)	Level A
MD_DW_LIN36	MD II (no MD III or MD IV)	Level A

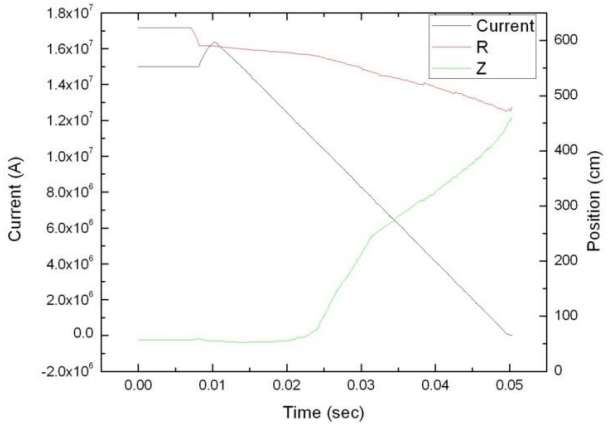

Figure 3 Plasma current and position during major upward disruption with 36 ms linear decay.

Figure 3 presents the total plasma current and its center position during major upward disruption with a 36 ms linear current decay, which is the most important disruption case that gives the largest radial moment.

IV. Eddy Current Distribution

Figure 4 presents the EPP eddy current distribution at the end of the major upward disruption with a 36 ms linear decay of plasma current. The primary eddy current loops are 1) one big horizontal loop in the front part of each DFW/DSM, and front half of each vertical drawer 2) two big current loops on top and bottom of the EPP structure (not shown). The potential voltage of current loop on each drawer is estimated to be less than 25 V and the total current flowing in each eddy loop is over 100 kA.

The net current induced on the VV is slightly less than the 15 MA plasma current mainly due to the conductive heat loss of the VV.

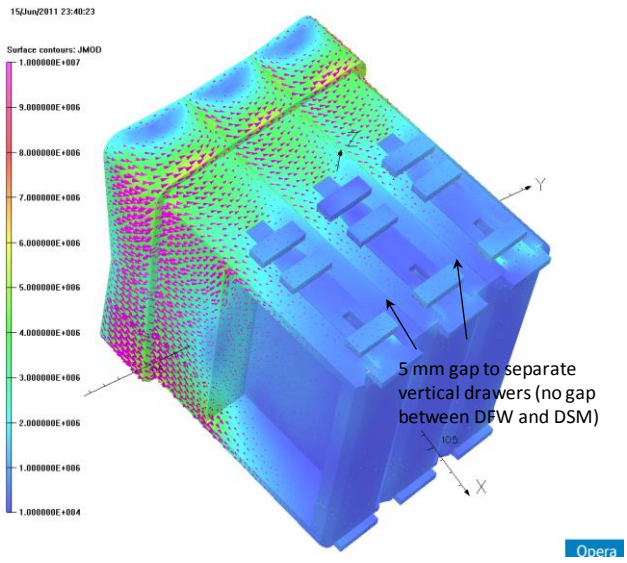

Figure 4 Eddy current in DFWs and DSMs during MD_UP_LIN36.

The model global behavior indicates that the eddy current appears on the inner VV wall first before penetrating to the outer wall and the induced current is in the same direction as the plasma current flowing direction as we expected during plasma quench. Table 3 shows current, voltage and net energy loss during major disruption on the EPP structure components.

Table 3 Current/voltage and net loss of the EPP structures

	Current (kA)	Voltage (V)	Loss (kJ)
DFWs/DSMs	100-150	25	450
Rails	10-30	2	5-6
EPP Structure	135	5	60

VI. Disruption Loads

Eddy current induced forces are the volume integration of JxB force for each structural component. Since the full EPP structure is bolted at the end of the rear flange, the net disruption moment is given at the center of rear flange of the EPP structure with radial and poloidal coordinates rc=11.5075 m and zc=0.62 m respectively.

Figure 5 presents a summary of peak EM loads on the full EPP structure for disruption scenarios listed in Table 2. Major disruption produces the largest radial force and radial moment on DFWs and the vertical drawers, but other disruptions may produce larger minority loads such as vertical force and vertical moment. Unlike the radial moment all other load components change polarity during disruptions.

To minimize the electrical contact, a radial gap between the DFWs and the vertical drawers will reduce disruption loads on the DFWs and the full EPP structure. Radial force on the full EPP structure is reduced by 40% with a gap and radial moment on the full EPP structure is reduced by 20%.

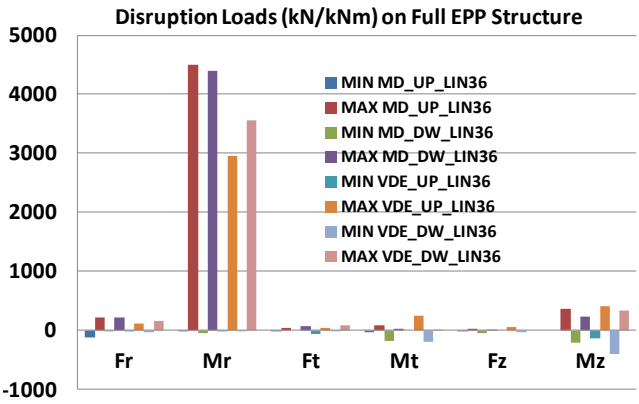

Figure 5 Disruption force and moment on the EPP for four disruption cases

Table 4 presents a summary of peak EM loads on the vertical drawers during plasma disruptions and VDEs. The moment for each drawer is given at the mass center of the vertical drawer. Radial moment is still dominant, but the poloidal force is more significant than the radial force. The disruption forces on the two side vertical drawers tend to compensate each other, particularly for the radial and poloidal forces.

Table 4 Total force and moment on EPP vertical drawers

	Net Force (kN)	Net Moment (MNm)
VDE_UP_LIN36	212	0.68
VDE_DW_LIN36	231	0.85
MD_UP_LIN36	270	1.13
MD_DW_LIN36	262	1.09

A clearance gap between DFWs and DSMs has an important impact on the EM loads (both on the DFWs and on the full EPP structure). The radial force on DFWs is reduced by a factor of 3; the radial moment is reduced by 18%, and the poloidal force is reduced by a factor of 2. Figure 6 listed the peak force and moment on DFWs during the major disruptions and VDEs.

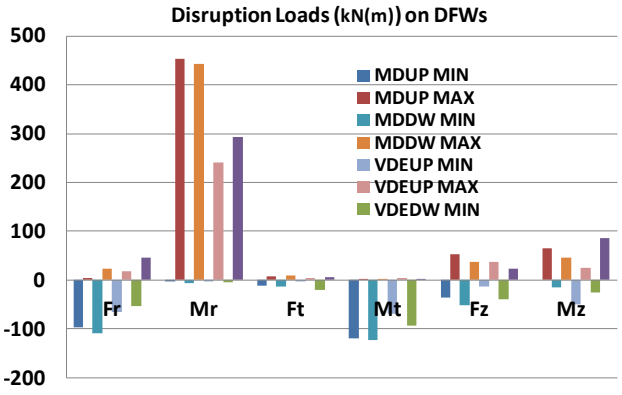

Figure 6 Disruption force and moment on the DFWs

VII. Response Implications

The design concept of DFW attachment scheme and mechanical integration of the DFWs with the drawers and EPP structure is validated by static and dynamic response analysis. The DFWs are supported at interface with DSMs via keys and pads; the DSMs are supported on the EPP structure via the sliding rails, bolts and pins. The EPP structure is cantilevered at the port plug rear flange. A full dynamic analysis indicates a dynamic amplification factor of ~1.2 [1]. The EPP structure is simply twisted under the dominant radial moment on the full EPP structure. The ~2 mm maximum deflection under the EM load only in the front face of DFWs is over a factor of 2 smaller than that from the horizontal drawer model due to the EM load reduction.

VIII. Currents on Rails, Keys and Water Pipes

To avoid local arcing and welding and to reduce EM force on water pipes, it is recommended to insulate the water pipes and diagnostic components from the DSM and EPP structure with ceramic coating. Disruption loads depend on eddy current flowing patterns on these components. An electrically insulated component will have a self-contained eddy current flowing pattern. For example, EM forces due to eddy current flowing on the front face of the DFWs tend to cancel out the forces due to returning eddy current flowing on the back surface. As a result, the net EM forces are smaller than the case of DFWs with large current transfer between DFWs and DSMs due to electrical contact. The moment arm length in a self-contained eddy current loop is also smaller than that of a large global eddy current loop.

Due to the electrical contact with the EPP structure, eddy current flowing in the rails, pins/keys and DSM water pipes will not form a self-contained loop and this will potentially increase the net EM loads on these EPP components.

A large amount of eddy current (10~30 kA) can flow in the bottom keys of the sliding rails during disruption, but only over a very short time frame. We need, however, to study potential welding at contact points between DSM and the rails in future work.

If no electrical contact with the EPP structure, there will be self-contained current loops on the vertical section of the water pipes and as a result, much smaller net EM loads (the pipes are largely self-supported). With contact, however, large amount of eddy current (0.2-0.3 kA) on EPP back plate leaks into the pipes during disruptions and thus significantly increase loads on the pipes (0.3-0.6 kN).

IX. CONCLUSIONS

The design of diagnostic EPP has changed from the horizontal drawer configuration to a vertical drawer configuration to effectively cut eddy current flowing paths on the EPP diagnostic drawers. As a result, a factor of 2-3 reduction of disruption loads brought down the deflection of EPP structure during disruptions. Although major disruption produces the largest radial moments and radial forces on the vertical drawers and the full EPP structure, other disruption cases or VDEs can produce larger poloidal moment and force as shown in Figures 5 and 6. The dominant radial moments do not tend to change polarity during disruption and VDE but all other load components do.

ACKNOWLEDGMENTS

This work is supported by DOE contract numbers DE-AC02-09CH11466 (PPPL) and DE-AC05-00or22725 (UC-Battelle, LLC). The views and opinions expressed herein do not necessarily reflect those of the ITER Organization.

REFERENCES

1. C. S. Pitcher et al, "Port-Based plasma diagnostic infrastructure on ITER", TOFE-2012, to be published in Fusion Science and Technology, 2012.
2. L. Doceul et al, "CEA engineering studies and integration of the ITER diagnostic port plugs", Fusion Engineering and Design, **82** 1216-1223, 2007.
3. L. Meunier et al, "Engineering activities on the ITER representative diagnostic equatorial port plug", Fusion Engineering and Design, **84** 1294-1299, 2009.
4. Y. Zhai et al, "Diagnostic equatorial port plug transient electromagnetic analysis during plasma disruptions and VDEs", ITER Report 4KXA57 v1.1, July, 2011.
5. A. Brooks, "EM analysis of the generic upper port plug diagnostic", ITER Report 348DL, May, 2010.

The Princeton Plasma Physics Laboratory is operated
by Princeton University under contract
with the U.S. Department of Energy.

Information Services
Princeton Plasma Physics Laboratory
P.O. Box 451
Princeton, NJ 08543

Phone: 609-243-2245
Fax: 609-243-2751
e-mail: pppl_info@pppl.gov
Internet Address: http://www.pppl.gov